

Mechanical behavior of shark vertebral centra at biologically relevant strains

Authors: ¹Ingle DI, ²Natanson LJ, ¹Porter ME

Keywords: mineralized cartilage, stiffness, toughness, double cone, elasmobranch

Affiliations:

¹ Florida Atlantic University, Boca Raton, FL 33431

² National Marine Fisheries Service, Narragansett, RI 02882

Author for correspondence: Danielle N. Ingle; Email: dingle2014@fau.edu

ABSTRACT

Cartilaginous shark skeletons experience axial deformation at the intervertebral joints, but also within the mineralized cartilaginous centrum, which can compress to between 3 - 8% of its original length in a free-swimming shark. Previous studies have focused on shark centra mechanical properties when loaded to failure, and our goal was to determine properties when compressed to a biologically relevant strain. We selected vertebrae from six shark species and from the anterior and posterior regions of the vertebral column. Centra were x-radiographed to measure double cone proportion and apex angles, and were mechanically tested at three displacement rates to 4% strain. We determined the variation in toughness and stiffness of vertebral centra among shark species, ontogenetic stages, testing strain rates, and compared anterior and posterior regions of the vertebral column. Our results suggest that toughness and stiffness, which are positively correlated, may be operating in concert to support lateral body undulations, while providing efficient energy transmission and return in these swift-swimming apex predators. We analyzed the contribution of double cone proportion and apex angles to centra mechanical behavior. We found that the greatest stiffness and toughness were in the youngest sharks and from the posterior body, and there was significant interspecific variation. Significant inverse correlations were found between mechanical properties and double cone apex angles suggesting that properties can be partially attributed to the angle forming the double cone apex. These comparative data highlight the importance of understanding cartilaginous skeleton mechanics under wide variety of loading conditions representative of swimming behaviors seen in the wild.

INTRODUCTION

In a swimming fish, the vertebral column is subjected to bending forces (compression and tension), which propagate a wave that increases in amplitude along the body axis (Long and Nipper, 1996). This wave originates approximately at the first dorsal fin or can be highly localized at the caudal peduncle, depending on species and swimming speed (Gemballa et al., 2006; Webb, 1975). Variations in body wavelength are likely influenced by vertebral column mechanical behavior (Porter et al., 2014; Donley et al., 2004; Long et al., 1994). In the cartilaginous vertebral column of sharks, strain (structural deformation) occurs not only at the intervertebral joints, but also within individual centra, allowing the entire vertebral column to engage as a spring at high tailbeat frequencies and shift into a brake at low tailbeat frequencies (Porter et al., 2016; 2014). The combination of strain occurring both within centra and at intervertebral joints results in greater total deformation along the vertebral column in cartilaginous fish when compared with their bony fish counterparts, and allows for greater elastic energy storage (Porter et al., 2014).

Previously considered a flimsier skeletal material than bone, mineralized cartilage of the vertebral column not only meets the mechanical demands of undulating sharks, but serves as a lighter alternative (Porter et al., 2016; 2014; 2007; 2006; Long et al., 2011; Porter and Long, 2010; Vogel, 1988). Mechanical properties of the shark vertebral column vary within individuals, between individuals, and among species (Porter et al., 2007; 2006). When vertebral column sections of a blacktip shark (*Carcharhinus limbatus*) and bonnethead shark (*Sphyrna tiburo*) were bent *ex vivo*, the magnitude-dependent elastic response was highest in the posterior regions and differed between species, while the time-dependent viscous response varied among species only (Long et al., 2011). Using sonomicrometry, *in situ* and *in vivo* strains were measured in the vertebral columns of spiny dogfish (*Squalus acanthias*). In preparations of multiple centra connected by joints and isolated centra, strain varied among individuals and swimming behaviors. During volitional swimming trials, isolated centra compressed 3-8% of their original length, while

segments consisting of two centra connected by one intervertebral joint compressed up to 30% of the original segment length (Porter et al., 2014). These studies highlight the importance of understanding interspecific variation of the mechanical behavior of mineralized shark cartilage at biologically relevant strains.

Shark vertebrae are cylindrical structures (centra) with neural arches that project dorsally. In the caudal region, vertebrae also have hemal arches that project ventrally (Fig. 1). A centrum consists of an areolar mineralized double cone structure (concentric rings that extend outward from the central apex) that is surrounded by both mineralized and unmineralized phases of cartilage (Fig. 1; Porter and Long, 2010; Dean and Summers, 2006; Ridewood, 1921). Greater mineral content has been shown to significantly increase centrum stiffness and strength (Porter et al., 2007). The amount and arrangement of this mineralization can vary among species, ontogenetically, and within an individual (Newberry et al., 2015; Porter et al., 2007; 2006; Cailliet and Goldman, 2004; Dingerkus et al., 1991; Urist, 1962; Ridewood, 1921). For example, Carcharhiniformes have double cones made of densely calcified wedges that stretch between opposing arms of corpus calcarea to form the intermedialia, while Lamniformes have radiating lamellae with a less calcified intermedialia (Fig. 1; Natanson et al., 2018; Newberry et al., 2015; Ridewood, 1921). These data are congruent with Porter *et al.* (2006), which found that the sandbar shark (*Carcharhinus plumbeus*), silky shark (*Carcharhinus falciformis*), and smooth hammerhead (*Sphyrna zygaena*), all Carcharhiniformes species, had almost 10% greater mineral content than the shortfin mako (*Isurus oxyrinchus*), a Lamniformes shark. Centrum mineral deposits asymptotically, and growth increases throughout life until a threshold is reached (Dingerkus et al., 1991). Ontogenetic changes in the calcified skeleton have been found in the bonnethead shark, *S. tiburo*. At maturity, males exhibit an anterior cephalic “bulge” from the three elongated rostral cartilages that develop in concert with the elongation and calcification of the claspers (Kajiura et al., 2005). Mineralization of the axial skeleton varies intra-individually in the

vertebrae of the deep-dwelling Greenland shark (*Somniosus microcephalus*), which are almost completely uncalcified except for those closest to the caudal fin (Ridewood, 1921). A comparative study, which investigated centra from the same animals sampled for the present study, found that shark centra band pair deposition and vertebral growth have strong positive correlations with body girth, which varies regionally along the vertebral column (Natanson et al., 2018). Greater band pair deposition, in concert with more mineral content, may have implications for vertebral mechanical behavior among and within undulating sharks.

Previous work on cartilaginous fish skeletal mechanics has focused on vertebral behavior at failure (Porter and Long, 2010; Porter et al., 2007; 2006). Shark centra stiffness, which ranges between 26 – 564 MPa, is similar to the stiffness of mammalian vertebral trabecular bone (76 - 352 MPa) (Porter et al., 2006; Banse et al., 2002; Swartz et al., 1991). Centra appear to have two major failure patterns: a shearing break between the apices of the mineralized double cone or by fracture within a single cone (Fig. 1; Porter et al., 2007). The role of the cartilaginous arches may be to distribute stress along the vertebral column rather than bearing major loads during locomotion (Porter and Long, 2010). However, these mechanical data do not represent typical non-destructive *in vivo* behavior in a volitionally swimming shark. We aim to quantify mineralized cartilage compressive behavior within a centrum's elastic region, or before permanent deformation has taken place.

The present study explores centra mechanical properties (stiffness and toughness) in six shark species, within two orders (Carcharhiniformes and Lamniformes); species were chosen for their differing body and vertebral morphologies. Carcharhiniformes inhabit coastal, inshore, and offshore waters, and they have a heterocercal caudal fin and a flattened head (Compagno, 2003). Their vertebral centra are mineralized with characteristic “solid” pie-shaped wedges (Natanson et al. 2018; Thomson and Simanek 1977; Ridewood 1921). In contrast, Lamniformes habitats range from shallow waters to the pelagic ocean, and they often have a tunniform shape with a

homocercal caudal fin for high-performance swimming, such as the shortfin mako (*Isurus oxyrinchus*) (Compagno, 2001). An exceptional Lamniformes is the common thresher shark, which has a bullet-shaped body with a heterocercal tail, of which the top portion is approximately half its total length. Lamniformes have “septate” centra with radiating lamellae and generally obtain a larger size than Carcharhiniformes (Natanson et al. 2018; Ridewood 1921).

Our first goal was to examine interspecific, regional, and developmental variations of centra mechanical properties when compressed to a biologically relevant strain. Specifically, we quantified stiffness (resistance to deformation) and toughness (ability to absorb energy) of centra strained to 4% of original length as a proxy for the material deformation that occurs in volitional swimming (Porter et al., 2014). Our second and third goals were to: (2) quantify mineral content and angles formed at the apex of the mineralized double cone structure within each centrum, and (3) determine if variation in mineralized double cone proportions and apex angles significantly correlate with centra properties (stiffness and toughness). Since mineral is highly concentrated within the double cone, we examined the proportion of double cone area relative to the total area of each centrum as a non-destructive estimate of mineral content. However, more dispersed mineral does occur outside the double cone structure.

We hypothesized that stiffness, toughness, and double cone proportion would be greatest in mature animals because sharks deposit mineral and lay down band pairs with growth (Natanson et al., 2018; Kajiura et al., 2005; Dingerkus et al., 1991). We hypothesized that posterior regions of the vertebral column to have greater mechanical properties and double cone proportion to support the high forces that translate to the tail during locomotion compared with vertebral regions near the head (Porter et al., 2007; Gemballa et al., 2006; Donley et al., 2004; Long and Nipper, 1996; Webb, 1975). Carcharhiniformes exhibit dense calcification within centra, and we hypothesized species of this order would have greater stiffness and toughness and a greater proportion of the double cone structure compared with Laminiformes (Porter et al., 2006).

We also proposed that the angles forming the apices of the mineralized double cones would contribute to mechanical behavior (Porter and Long, 2010). Finally, we consider results of this study in light of an investigation of shark vertebral morphology and body shape (Natanson et al., 2018).

MATERIALS AND METHODS

Experimental animals

Vertebrae were sampled from two orders (Carcharhiniformes and Lamniformes) and three families (Carcharhinidae, Lamnidae, and Alopiidae) of sharks. Carcharhiniformes including the dusky shark (*Carcharhinus obscurus*: Carcharhinidae) and blue shark (*Prionace glauca*: Carcharhinidae). Lamniformes including the white shark (*Carcharodon carcharias*: Lamnidae), shortfin mako (*Isurus oxyrinchus*: Lamnidae), porbeagle (*Lamna nasus*: Lamnidae), and common thresher shark (*Alopias vulpinus*: Alopiidae). Species will be referenced using their common names throughout this manuscript (Table 1).

Sampling

Shark specimens were collected from sport-fishing tournaments, research cruises, strandings, and commercial fishermen in the western North Atlantic Ocean. Specimens were usually frozen within four hours of collection. In most cases vertebrae were collected within a few hours of death, however, in the case of a stranding, specimens may have been dead a longer period of time. From each shark, three of each set of adjacent vertebrae were prepared for mechanical testing, and two were used for x-radiography and vertebral morphology related to ageing in a companion study (Natanson et al., 2018).

We obtained a small (young of the year: YOY), mature, and immature shark from each species (Table 1). We maintained ontogenetic consistency based on individual species growth

curves (dusky (Natanson et al., 1995); blue shark (Skomal and Natanson, 2003); common thresher shark (Gervelis and Natanson, 2013); porbeagle (Natanson et al., 2002); shortfin mako (Natanson et al., 2006); and white shark (Natanson & Skomal, 2015). Although developmentally intermediate sharks are much closer in length to mature animals than the YOY within a species, centra from animals that have not yet reached physical maturity may differ mechanically from their mature counterparts (Table 1). There was overlap in the individual fork lengths among species that resulted in similar lengths within the immature and mature ontogenetic groupings, with the exception of the much larger white shark. In addition, white sharks, shortfin makos, and common thresher sharks were approximately twice the length of dusky, blue, and porbeagle specimens (Table 1).

From all six species, vertebrae were obtained from four locations along the body, which denoted two regions (anterior and posterior) (Fig. 2). In each location, three adjacent vertebrae were prepared for mechanical testing. Vertebrae from the anterior (pre-caudal) region were located at the insertion of the pectoral fins and at the origin of the first dorsal fin; while vertebrae from the posterior (caudal region) were located at the origin of the second dorsal fin, and at the pre-caudal pit. In total, we obtained 12 vertebrae from each individual ($n = 3$ per species). Natanson *et al.* (2018), who sampled from the same locations of the vertebral column, further validated our anterior/posterior assignments since there was no significant difference in body girth between where the pectoral fins insert and the location in which the first dorsal fin originates, as well as no differences in girth between the origin of the second dorsal fin and pre-caudal pit.

Mechanical properties

Samples were freshly frozen when extracted from the vertebral column; previous research has shown that the mechanical properties of frozen tissue are not altered (Panjabi et al., 1985). We thawed vertebrae and removed neural and hemal arches with standard dissection equipment (Fig. 1). We measured centra length and diameter (mid-transverse plane across lateral aspects

of each centrum) with digital calipers to the nearest 0.01mm and cross-sectional area was calculated to the nearest 0.01mm². We then placed centra in elasmobranch Ringer's solution for 2 h prior to mechanical testing. We used an E1000 Instron mechanical tester with a 2kN load cell to compress centra in the rostro-caudal axis. All centra were pre-loaded to 5N to minimize shifting of the sample between platens in the toe region of the stress-strain curve. Quasi-static compression tests did not transition from elastic to plastic deformation during loading, with the exception of one vertebra from a YOY blue shark; therefore, centra were not permanently deformed and returned to their original shape when unloaded. Within each anatomical region, we tested each centrum at one of the three following strain rates: 0.1%, 1%, and 10% (centrum length) per second. Centra lengths varied greatly; the smallest length was 2.6 mm from a YOY dusky, while the greatest length was 28.33 mm from a mature white shark (Table 1). We calculated strain rates based on percentage of averaged centra lengths within a group of adjacent vertebrae. Although the effect of various strain rates on elasmobranch cartilaginous vertebrae in compression to failure has been previously investigated, the potential effects of vertebral column region, individual size, or species were not considered at biologically relevant strains (Porter et al., 2007).

We tested 12 vertebrae from each individual in all six species; however, one vertebra each from a shortfin mako and white shark was excluded from testing due to tissue damage. Using the Instron system, stress and strain were calculated from load and displacement in Bluehill software. Stress was calculated by dividing the load by each centrum's cross-sectional area, and strain was calculated by dividing the centrum's change in length by the original length. Stiffness and toughness were determined from the stress-strain curves. We calculated stiffness as stress/strain at the point of 4% deformation of each centrum length, and toughness was determined as the area under the curve between 0%-4% strain (Figs. 3, S1). We selected 4% strain to as a standardized displacement to calculate mechanical properties based on strains occurring *in vivo* during swimming (Porter et al., 2014).

These mechanical tests come with two important caveats. Although we assumed tissue homogeneity within and among centra, which we standardized by cross-sectional area, there is large variation in mineral arrangement throughout these skeletal elements (Figs. 1, 4). Also, more research is required to understand the complexity of the interaction between heavily mineralized phases of cartilaginous centra with the unmineralized phases, which could be used to model load distribution within a centrum. Our second assumption was that the entire cross-sectional area of a centrum simultaneously bears the complete compressive load. In reality, the vertebral column is alternatively engaged in compression and tension during lateral displacement. Also, the loading rate is dependent on swimming speed; which likely varies dramatically among species and behaviors (feeding, mating, cruising, etc.) (Sfakiotakis et al., 1999; Lindsey, 1978).

X-radiographs

After mechanical testing, two centra from every shark (from the pectoral fin insertion and second dorsal fin origin) were x-radiographed in a sagittal orientation to show the double cone structure with a 20KHz high frequency machine (Figs. 1, 2, 4; model InnoVet™ Select, InnoVet™, Chicago, IL, USA). Most centra were imaged at 40KvP and 3.5mAs, but centra from larger sharks required varying these settings to obtain clear images of the mineralized cone structure. If modified, radiograph settings were held constant within an animal. In the YOY blue shark centrum that was permanently deformed during mechanical testing, an adjacent centrum (from the same shark and anatomical region) was used for imaging. The following measurements were made from the x-radiographs using Image J v1.45 (National Institute of the Health, USA): centra double cone area, centra total area, and angle measurements of the two cone's apices oriented towards each centrum center (Fig. 1). Double cone area was quantified by tracing the edge of the mineralized cone structures, at the boundary between the double cone outer edges and the surrounding cartilage. Total area was quantified by selecting the entire centrum (Fig. 1). Double

cone proportion was calculated by dividing double cone area by total centrum area. The angle measurement included in the statistical model was the angle average of the two cone apices.

Statistical analysis

Toughness, stiffness, double cone proportion, and double cone apex angle were discrete variables that failed the Anderson-Darling test for normality, and they were normal after being log transformed. We used a mixed model ANOVA ($P < 0.05$) to examine differences in centra stiffness and toughness using animal ontogenetic group, body region, species, and strain rate as the main effects in JMP v.5.0.1.a (SAS Institute Inc., Cary, NC, USA). We included interaction terms for all main effects, excluding the term ontogenetic group*species, since there would be only one individual for each categorization. Individuals for each shark species were assigned to one of the following three ontogenetic groups based on previously published growth curves for each species: young-of-the-year (YOY), immature, and mature. The body was divided into two regions: anterior (pectoral fin insertion and first dorsal fin origin) and posterior (second dorsal fin origin and pre-caudal pit). Strain rate (0.1%, 1.0%, and 10%) from each centrum was included in the model. Post hoc Tukey tests compared differences in mechanical properties within animal ontogenetic group, body region, species, and strain rate. A simple linear regression was used to evaluate the relationship between stiffness and toughness.

To examine the impact of centrum morphology (double cone proportion and apex angle) on mechanical properties (stiffness and toughness), we ran a multiple regression model ($P < 0.05$). These analyses included only a subset of data since only 36 of the centra were x-radiographed.

RESULTS

Mechanical properties

Our mixed model ANOVAs were significant for toughness ($F_{47,166}=10.8273$, $P<0.0001$; $R^2=0.754$) and stiffness ($F_{47,166}=7.7765$, $P<0.0001$; $R^2=0.6876$). Animal ontogenetic group, body region, species, and strain rate were significant effects for both toughness and stiffness ($P<0.001$). In the toughness and stiffness models, the significant interaction effect was region and species ($P<0.01$). Below we outline the *post-hoc* results for the significant main effects.

Ontogenetic group was a significant effect ($P<0.001$) for toughness and stiffness. Centra from YOY sharks were the toughest, mature sharks were the least tough, and immature sharks had intermediate centra toughness (Fig. 5A). Centra from YOY sharks were stiffest while the mature sharks were least stiff and immature sharks were intermediate (Fig. 5B).

Region and species were significantly main effects ($P<0.001$) and the species*region interaction term was also significant for toughness and stiffness ($P=0.0047$ and $P=0.0103$, respectively). Overall, centra from the posterior region (second dorsal fin insertion and pre-caudal pit) were significantly tougher than the anterior region (pectoral fin insertion and first dorsal fin origin), and the dusky and blue sharks had the toughest centra of all species (Fig. 6A). Specifically, posteriorly-located centra from the dusky shark, shortfin mako and white shark were significantly tougher than in the anterior body. Centra from the posterior region were significantly stiffer than those from the anterior region, and dusky shark had stiffer centra than all other species (Fig. 6B). When regional variation was considered for each species, only the dusky shark and shortfin mako had significantly stiffer centra in the posterior body when compared to the anterior body.

Strain rate was a significant effect ($P < 0.001$) in the toughness and stiffness models. Mechanical tests using faster strain rates (10% of centrum length; mm/s) on cartilaginous vertebrae resulted in greater toughness than the slower rates of displacement (Fig. 7A). In our *post hoc* comparisons, centra were significantly stiffer at 10% strain rate compared to 1.0% and 0.1% strain rates (Fig. 7B).

The relationship between toughness and stiffness was strongly positive. In addition, two-fold increases in stiffness resulted in proportional increases in toughness ($R^2 = 0.825$, $P < 0.0001$; Fig. 8).

X-radiographs

Our multiple regression model for toughness was significant ($F_{32,35} = 3.072$, $P = 0.042$) and double cone apex angle was the only significant effect ($P = 0.007$). We used simple regressions to show a significant inverse relationship between toughness and double cone apex angle ($R^2 = 0.1749$, $P = 0.0111$; Fig. 9A). Similarly, we used a multiple regression model to examine the impacts of double cone proportion and apex angle on centrum stiffness ($F_{32,35} = 2.885$, $P = 0.051$) and apex angle was a significant effect ($P = 0.0075$). We used simple linear regressions to show an inverse relation between stiffness and double cone angle apex ($R^2 = 0.1825$, $P = 0.0094$; Fig. 9B).

DISCUSSION

We found that mechanical properties of cartilaginous shark centra, when deformed to a biologically relevant strain, vary among ontogenetic group body region, species, and also exhibit viscoelastic behavior (Figs. 5, 6, 7). Our results suggest that mechanical toughness and stiffness,

which have a strong positive relationship, may be operating in concert to support lateral body undulations, while providing efficient energy transmission and return in swimming sharks (Fig. 8). We proposed that variation in mechanical properties can be, in part, attributed to the proportion of mineralized double cone and double cone apex angles that build the internal framework of load-bearing centra. While we found no significant correlation between mechanical properties and double cone proportion, we did detect significant relationships between properties and double cone apex angles (Fig. 9).

Mechanical properties

Centra mineral deposits asymptotically and with maturity. Mineral content has been previously shown to correlate with stiffness and toughness, therefore we expected centra from mature animals to have a greater ability to resist deformation and absorb energy (Porter et al., 2007; 2006; Kajiura et al., 2005; Dingerkus et al., 1991). Contrary to our hypothesis, YOY sharks had the stiffest and toughest centra (Table S1; Fig. 5). Our data suggest that the transitional boundary between the mineralized double cone and surrounding cartilage in centra may vary with development, impacting the amount of the mineralized phase being compressed at 4% strain among ontogenetic groups. Specifically, we propose that the deformation seen in the youngest sharks recruited more of the mineralized phase than in the immature and mature animals (Figs. 4, 5). Our selection of 4% strain as a standardized displacement was informed by Porter *et al.* (2014), where compressive strain was measured *in vivo* in individual centra of volitionally swimming spiny dogfish (*S. acanthias*). However, a smaller (73.5-79 cm), benthic species (order Squaliformes) was used in that study, which was in the size range of the present study's smallest dusky and blue sharks (Table 1). It is possible that *in vivo* strain may differ among species with varying swimming styles and size ranges, for example, the orders Carcharhiniformes and

Lamniformes in this study. However, it would be difficult to measure *in vivo* mechanical behavior of these larger, faster swimming species in a laboratory setting.

As hypothesized, centra from the posterior region of the vertebral column were more stiff and tough than the anterior region (Fig. 6A). Greater toughness at biologically relevant strains indicated that centra would absorb more energy, potentially facilitating elastic recoil and the associated energy return. This mechanism is especially important in the posterior body where the greatest undulation is occurring (Gemballa et al. 2006). In general, stiffer skeletal elements will transfer energy more efficiently at all swimming speeds (Gemballa et al. 2006; Donley et al. 2004; Long & Nipper 1996; McHenry et al. 1995; Webb 1975). The regional variation in stiffness found here may transfer energy resulting in the largest lateral amplitude of the body axis occurring in the posterior region (Figs. 4, 6B).

Regional variation in mechanical properties may reflect differences in mineralization along the vertebral column. Mineralization found only in the caudal vertebral column of the Greenland shark (*Sommiosus microcephalus*) appears to reflect its behavioral ecology as a large and slow-swimming elasmobranch inhabiting deep, cold waters (Ridewood 1921). Natanson *et al.* (2018), using centra from the same specimens as this study, found regional variation among centra in centra size and band pair counts. Centra with the greatest volume and the most band pairs were found in the region of the vertebral column aligned with the abdominal cavity (largest body girth), while the smallest volume and number of band pairs were found near the head and caudal peduncle (smaller body girths). Since centra aligned with the abdominal cavity are within the anterior region and the posterior region had significantly greater stiffness and toughness, increased band pair counts may not correlate with greater centra mechanical properties of sharks found in the present study (Figs. 2, 6). Rather, more band pairs may reduce stiffness and toughness since the translucent bands may break up mineralization throughout the structure, resulting in a lower proportion of calcified tissue. In Lamniformes centra, rostrocaudal increases

in bifurcations and radial lamellae along the vertebral column may be contributing to the greater stiffness and toughness found in the posterior region of these species (Natanson et al., 2018). Since there is great diversity in shark morphology, swimming modes, and physiology, there is also variability in growth, mineralization, and mechanical properties found in their vertebrae.

Cartilaginous shark centra, like many biological materials, can have viscoelastic properties under variable loading regimes (Porter et al., 2007; Vogel, 2003; Vogel, 1988; Wainwright et al., 1976). To quantify the viscoelastic effects of cartilage, we tested shark centra in quasi-static compression at three different strain rates (distance traveled per second), which were calculated as 0.1%, 1%, or 10% of a centrum length. Centra were toughest at the fastest strain rate (10%) suggesting that at faster swimming speeds, sharks can store a greater amount of energy that may be returned to the undulating body (Fig 7A). Porter *et al.* (2007) reported no change in stiffness at failure with changing strain rates; however, we found that centra were stiffer at faster strain rates when tested at biologically relevant strains (Fig. 7B). Due to these incongruent findings, we suggest the viscoelastic effects of mineralized cartilage and vertebral columns should continue to be explored among a range of testing conditions and species. For example, we found that stiffness did not change for the mature common thresher shark centrum, but stiffness did drop slightly in the mature dusky shark centrum during testing (Fig. S2).

There is generally an inverse relationship between stiffness and toughness in biological materials. A material's brittleness increases with stiffness, lowering the material's ability to absorb energy, resulting in easier fracture (Currey 1999). The relationship between these properties may mediate the mechanics of the undulating axial skeleton of a swimming shark while maintaining the structural integrity of the vertebral column. We found a strong positive regression with the ability of shark centra to absorb energy (toughness) and mechanical resistance to deformation (stiffness; Fig. 8). If the amount of deformation were held constant during quasi-static compression, a greater slope (stiffness) of the initial linear portion of the stress-strain curve would

occur in tandem with a greater area under the curve (toughness) (Figs. 3, S1). These data show that centra can resist deformation and absorb energy when compressed within the material's elastic region (before permanent deformation has taken place).

X-radiographs

We hypothesized that centra with greater stiffness and toughness would have a greater proportion of the mineralized double cone. We found no significant relationship between double cone proportion with either toughness or stiffness. Since mineral morphologies were analyzed non-destructively in 2D x-radiographs, the double cone proportion measurement may have excluded load-bearing calcified structures that contribute to the centra's mechanical behavior. For example, carcharhinid double cone morphology is wedge-shaped and densely packed with mineral, while lamnids have thin, radiating lamellae that extend outward from the double cone structure and may contribute to centra mechanical properties (Fig. 4). With 2D analyses, it is difficult to separate out and quantify these calcified structures from the surrounding cartilage. Although we found no relationship between cone proportion and mechanical properties, previous data supports that mineral content and arrangement both contribute to a biological material's behavior when loaded (Porter et al. 2007; Currey 1984). It is possible that a different imaging tool, such as micro-computed tomography, may be better equipped to quantify and analyze the intricacies of the double cone morphology and the calcification that extends outward from the double cone structure (Fig. 4). With a more comprehensive structural analysis, the mechanical contribution of mineral surrounding the double cone can be considered.

Previous research showed that dislocating cone apices was the most common fracture pattern at failure in mineralized cartilaginous centra (Porter and Long, 2010). We hypothesized that since this type of fracture was common at failure, the angle of the apices would significantly

impact mechanical properties in biologically relevant testing in the elastic region. Our data did not significantly link mineral arrangement with mechanical properties. We found inverse relations between mechanical properties and cone apex angle (Fig. 9). With a smaller angle formed at the apex of each cone, the distance between corpus calcarea of opposite cones would be greater potentially providing a rigid structure capable of more energy storage than if the apex angles were larger (Fig. 1, 4).

Ecological implications

Historically, the alternating patterns of mineralization in elasmobranch vertebral centra have been counted and used as a proxy for age. However, it has become clear that these patterns are not related to time (Harry, 2017). The current study was designed in conjunction with Natanson et al. (2018) to understand the relationship of band pair deposition to age, growth and/or structure, and the influence these characteristics have on the mechanical behavior of vertebral elements. These studies are further strengthened by the sampling of adjacent vertebrae from the same individual sharks from the six species examined here.

We hypothesized that in swimming sharks, variation in vertebral morphology results in differences in the mechanical behavior of the vertebral column, and that variations are most apparent between Orders Carcharhiniformes and Lamniformes. In Natanson et al. (2018), species-specific relationships among band pair count, fork length, girth, and centrum volume demonstrated a structural relationship between cross-sectional body shape and vertebral morphology within and among species and ontogenetically, which suggest that centra provide a supportive role in the shark body. Since there is great diversity in shark morphology, swimming modes, and physiology, there is also variability in growth and mineralization of the vertebrae. Data from Natanson et al. (2018) showed that species of similar body shapes and swimming modes

also had similar vertebral morphological characteristics. An extreme example demonstrating the relationship of body shape to vertebral morphology is the common thresher shark, in which vertebral size was largest mid-body and maintained this size up to the beginning of the tail. The common thresher shark depends heavily on its tail for stunning prey when feeding, thus the relationship between vertebral size and body location may reflect this dependence on a strong and long tail (Oliver et al. 2013). Essentially, the common thresher body maybe operating as a whip, which may require low stiffness and toughness to achieve that level of flexibility (Fig. 6). Centra from other Lamniformes, specifically the shortfin mako, porbeagle, and white shark, also showed increases in bifurcations of the radiating lamellae that were related to size, suggesting that vertebrae need additional support as they grow (Natanson et al. 2018). This idea is corroborated by the data presented here; Lamniformes vertebrae had lower stiffness and toughness than Carcharhiniformes (Fig. 6).

We also hypothesized that alternating mineralization patterns (band pairs) relate to stiffness and toughness of the centra as a response to external forces on the vertebrae. As body shape changes drastically near the tapered caudal region, differences in body shape, vertebral morphology and muscle arrangement would differentially affect vertebral loading along the column (Natanson et al. 2018; Gemballa et al, 2006). Species and ontogenetic differences in body shape and locomotor style will also impact the vertebral loading regime, and deposition of each band type may depend on location along the column, species, and life history. We found that in mature sharks, the greatest toughness and stiffness often had the lowest number of band pairs, and counts were consistently lowest in posterior regions within an individual and in the Carcharhiniformes (Table Sa1; Natanson et al., 2018). Bands are translucent unmineralized tissue dispersed concentrically throughout the double cone structure, the load bearing component of the centra (Porter et al., 2006; 2007). More bands may break up and reduce the mineralization in the double cone, and decreasing mineral in the centra has been shown to decrease stiffness

(Porter et al., 2007). For example, Porter *et al.* (2007) found decreased stiffness in demineralized centra, suggesting that the mineralized component is necessary for structural support. The results of the present study show that fewer band pairs in the posterior region may contribute to stiffness and facilitate force translation to the caudal region during swimming (Fig. 6B; Natanson et al. 2018).

One exception we found to the inverse relationships between band pair counts to mechanical properties was in the shortfin mako, which had stiff and tough centra and the highest band pair counts compared to species (Fig. 6; Table S1; Natanson et al., 2018). This incongruity may be due to increased birufications and radiating lamellae, which distribute mineral throughout the centrum to support the high-speed swimming characteristic of the shortfin mako. The results of the current study, along with those of Natanson et al. (2018) suggest that there are different mechanical and structural needs depending on method of locomotion, animal size, and other musculoskeletal inputs that correspond to differences in body morphology (Fig. 5-8). In tandem, these investigations indicate that the alternating mineralized zones are related to structure and swimming mode rather than age.

Summary

In sharks, the vertebral column is governed by dynamic and complex interactions among tissue composition and morphology. We examined the compressive mechanical properties at a biologically relevant strain (4%) and assessed mineral arrangement of vertebral centra in six shark species. We found that mechanical properties (stiffness and toughness) vary among ontogenetic group, body region, strain rate, and species. Before permanent deformation, centra have a proportional ability to resist changes in shape and absorb energy. We found no relationship between centra mechanical behavior and the amount of mineralized double cone composing the centra, our proxy for mineral content. However, we did detect significant inverse relationships

between central mechanical properties and angles formed at the double cone apex. We propose that with higher resolution 3D imaging, calcified structures contributing to mechanical behavior can be more comprehensively assessed and enhance our understanding of the form-function relationship in mineralized shark cartilage.

Acknowledgements. We thank R. McConkey, W. Nambu, Y. Kayan, C. Jackson, and K. Vidicuc for help with data collection and D. Serra for use of the x-ray equipment. We gratefully acknowledge the Marine Technology Society for funding. We also thank the fishermen who brought us samples or allowed us to sample their catches.

Competing interests. The authors declare that they have no competing interests.

Author's contributions. L.J.N. provided the samples. D.N.I., L.J.N., and M.E.P. designed the project goals. D.N.I. developed the methods and collected data. D.N.I. prepared earlier versions of the manuscript and all authors contributed to the final version.

Funding. This research was supported by the Marine Technology Scholarship to D.N.I.

Data accessibility. Raw data will be made available upon request. Summary data, in .xls format, are available on Dataverse. DOI:

References:

- Banse, X., Sims, T. & Bailey, A. (2002). Mechanical properties of adult vertebral cancellous bone: correlation with collagen intermolecular cross-links. *J Bone Miner Res*, 17(9), pp.1621–1628.
- Cailliet, G.M. & Goldman, K.J., (2004). Age determination and validation in chondrichthyan fishes. In *Biology of Sharks and Their Relatives* (eds. J. C. Carrier, J. A. Musick, & M. R. Heithaus), pp. 399–447. Boca Raton: CRC Press.
- Campbell, FC. (2008). *Elements of Metallurgy and Engineering Alloys*. ASM International.
- Compagno, L. (2003). *Sharks of the Order Carcharhiniformes*, Caldwell: Blackburn Press.
- Compagno, L.(2001). Sharks of the world. An annotated and illustrated catalogue of Shark species known to date. Volume 2. Bullhead, mackerel, and carpet sharks (Heterodontiformes, Lamniformes, and Orectolobiformes. *FAO Species Catalogue for Fishery Purposes*, 1(2).
- Currey, J.(1999). The design of mineralized hard tissues for their mechanical functions. *J Exp Biol*, 202, pp.3285–3294.
- Currey, J.(1984). *The mechanical adaptations of bones*, New Jersey: Princeton.
- Dean, M.N. and Summers, A.P.(2006). Mineralized cartilage in the skeleton of chondrichthyan fishes. *Zool*, 109, pp.164–168.
- Dingerkus, G., Seret, B. and Guilbert, E.(1991). Multiple primatic calcium phosphate layers in the jaws of present-day sharks (Chondrichthyes: Selachii. *Experimentia*, 47, pp.38–40.
- Donley, J.M. et al., 2004. Convergent evolution in mechanical design of lamnid sharks and tunas. *Nature*, 429, pp.61–65.
- Fouts, W. and Nelson, D.(1999). Prey capture by the Pacific angel shark, *Squatina californica*: visually mediated strikes and ambush-site characteristics. *Copeia*, pp.304–312.
- Gemballa, S., Konstantinidis, P., Donley, J.M., Sepulveda, C., and Shadwick, R.E. (2006). Evolution of high-performance swimming in sharks: transformations of the musculotendinous system from subcarangiform to thunniform swimmers. *J Morphol*, 267, pp.477–493.
- Gemballa, S. and Vogel, F. (2002). Spatial arrangement of white muscle fibers and myoseptal tendons in fishes. *Comp Biochem Physiol A Mol Integr Physiol*, 133(4), pp.1013–1037.
- Gervelis, B.J. and Natanson, L.J. (2013). Age and growth of the common thresher shark in the western North Atlantic Ocean. *Transactions of the American Fisheries Society*, 142, pp.1535-1545.
- Harry, A.V. (2017). Evidence for systemic age underestimation in shark and ray ageing studies. *Fish and Fisheries* doi:10.1111/faf.12243.
- Hebrank, J.H., Hebrank, M.R., Long, J.H., Block, B.A. and Wright, S.A. (1990). Backbone mechanics of the blue marlin *Makaira nigricans* (Pisces, Istiophoridae). *J Exp Biol*, 148(1), pp. 149-159.
- Lindsey, C. (1978). Form, function, and locomotory habits in fish. In *Fish Physiology*:

- Locomotion* (eds. W. Hoar and D. Randall) pp. 1-100, New York: Academic Press.
- Long Jr., J.H, Koob, T., Schaefer, J., Summers, A., Bantilan, K., Grotmol, S. and Porter, M.E. (2011). Inspired by sharks: a biomimetic skeleton for the propulsive tail of an aquatic robot. *Mar Technol Soc J*, 45(4), pp.119–129.
- Long Jr., J.H. and Nipper, K. (1996). The importance of body stiffness in undulatory propulsion. *Am Zool*, 36(678–694).
- Long Jr., J.H., McHenry, M. and Boetticher, N. (1994). Undulatory swimming: how traveling waves are produced and modulated in sunfish (*Lepomis gibbosus*). *J Exp Biol*, 192(1), PP.129-145.
- Mamlouk, M. and Zaniewski, J. (2011). *Mechanicals for civil and construction engineers* 3rd ed., Upper Saddle River: Pearson Education, Inc.
- MacNeil, M.A. et al. (2012). Biology of the Greenland shark *Somniosus microcephalus*. *J Fish Biol*, 80(5), pp. 991-1018.
- Natanson, L.J., Skomal, G.B., Hoffmann, S.L., Porter, M.E., Goldman, K.J. and Serra, D. (2018). Age and growth of sharks: do vertebral band pairs record age? *Mar Freshw Res*, 69(9) 1440-1452.
- Natanson, L.J. and Skomal, G.B. (2015). Age and growth of the white shark, *Carcharodon carcharias*, in the western North Atlantic Ocean. *Mar Freshw Res*, 66(5), pp.387-398.
- Natanson, L.J., Kohler, N.E., Ardizzone, D., Calliet, G.M. Witner, S.P. and Mollet, H.F. (2006). Validated age and growth estimates for the shortfin mako, *Isurus oxyrinchus*, in the North Atlantic Ocean. *Environ Biol Fish*, 77(3-4), pp.367-383.
- Natanson, L.J., Mello, J.J. and Campana, S.E. Validated growth of the porbeagle shark (*Lamna nasus*) in the western North Atlantic Ocean. *Fish Bull*, 100(2), pp.266-278.
- Natanson, L.J., Casey, J.G. and Kohler, N.E. (1995). Age and growth estimates for the dusky shark, *Carcharhinus obscurus*, in the western North Atlantic Ocean. *Fish Bull*, 93, pp.116-126.
- Newberry, M.G., Siverson, M., Cook, T.D., Fotheringham, A.M., and Sanchez, R.L. (2015). Vertebral morphology, dentition, age, growth, and ecology of the large lamniform shark *Cardabiodon ricki*. *Acta Palaeontologica Polonica*, 60(4), pp.877–897.
- Oliver, S., Turner, J.R., Gann, K., Silvosa, M., and Jackson, T.D.U. (2013). Thresher sharks use tail-slaps as a hunting strategy. *PloS one*, 8(7), p.e67380.
- Panjabi, M.M., Krag, M., Summers, D. and Videman, T. (1985). Biomechanical time-tolerance of fresh cadaveric human spine specimens. *J Orthop Res*, 3(3), pp.292–300.
- Porter, M., Ewoldt, R. and Long Jr, J. (2016). Automatic control: the vertebral column of dogfish sharks behaves as a continuously variable transmission with smoothly shifting functions. *J Exp Biol*, 219, pp.2908–2919.
- Porter, M.E., Diaz Jr., C., Sturm, J.J., Grotmol, S., Summers, A.P. and Long Jr., J.H. (2014). Built for speed: strain in the cartilaginous vertebral column of sharks. *Zool*, 117, pp.19–27.
- Porter, M.E., Beltran, J.L., Koob, T.J. and Summers, A.P. (2006). Mechanical properties and biochemical composition of mineralized vertebral cartilage in seven elasmobranch species (*Chondrichthyes*). *J Exp Biol*, 209, pp.2920–2928.

- Porter, M.E., Koob, T.J. and Summers, A.P. (2007). The contribution of mineral to the mechanical properties of vertebral cartilage from the smooth-hound cartilage *Mustelus californicus*. *J Exp Biol*, 210, pp.3319–3327.
- Porter, M.E. and Long Jr., J.H. (2010). Vertebrae in compression: mechanical behavior of arches and centra in the gray smooth-hound shark (*Mustelus californicus*). *J Morphol*, 271, pp.366–375.
- Ridewood, W.G. (1921). On the calcification of the vertebral centra in sharks and rays. *Philosophical Transactions of the Royal Society of London. Series B, Containing Papers of Biological Character*, 210, pp.311–407.
- Thomson, K.S., and Simanek, D.E. (1977). Body form and locomotion in sharks. *American Zoologist*, 17(2): 343-354.
- Sfakiotakis, M., Lane, D. and Davies, B. (1999). Review of fish swimming modes. *IEEE Journal of Oceanic Engineering*, 24, pp.237–252.
- Skomal, G.B. and Natanson, L.J. (2003). Age and growth of the blue shark, (*Prionace glauca*) in the North Atlantic Ocean. *Fish Bull*, 101, pp.627-639.
- Swartz, D.E., Wittenberg, R.H., Shea, M., White III, A.A. and Hayes, W.C. (1991). Physical and mechanical properties of calf lumbosacral trabecular bone. *J Biomech*, 24(11), pp.1059-1068.
- Urist, M. (1962). Calcium and other ions in blood and skeleton of Nicaraguan fresh-water shark. *Science*, 137, pp.984–986.
- Vogel, S. (2003). *Comparative biomechanics: life's physical world*, Princeton: Princeton University Press.
- Vogel, S. (1988). *Life's Devices*, Princeton: Princeton University Press.
- Wainwright, S. et al., 1976. *Mechanical Designs in Organisms*, New York: John Wiley & Sons.
- Webb, P.W. (1975). Hydrodynamics and energetics of fish propulsion. *Bull Fish Res Bd Can*, 190, pp.1–159.

Tables:

Table 1. Summary of fork lengths of YOY, immature, and mature animals of six shark species. The below information reports n=1 shark for each ontogenetic stage for every species

Species	Animal fork length (cm)			Average centrum length (mm)		
	YOY	Immat.	Mature	YOY	Immat.	Mature
Dusky shark (<i>Carcharhinus obscurus</i>)	74.5 M	211 F	226 F	5.29 ±0.12	14.85±0.47	15.89±0.64
Blue shark (<i>Prionace glauca</i>)	64.7 M	213 M	232 M	2.98±0.07	10.19±0.27	10.81±0.31
Shortfin mako (<i>Isurus oxyrinchus</i>)	141.5 M	203.1 F	291.5 F	8.24±0.36	10.62±0.44	15.38±0.41
Porbeagle (<i>Lamna nasus</i>)	89.6 F	204.1 F	218.2 F	5.64±0.15	13.99±0.49	15.45±0.54
Common thresher shark (<i>Alopias vulpinus</i>)	159.5 F	209.9 M	229 F	9.59±0.41	12.79±0.45	13.07±0.6
White shark (<i>Carcharodon carcharias</i>)	151.6 M	331 M	380.9 M	9±0.37	19.42±1.15	22.9±1.18

Figures

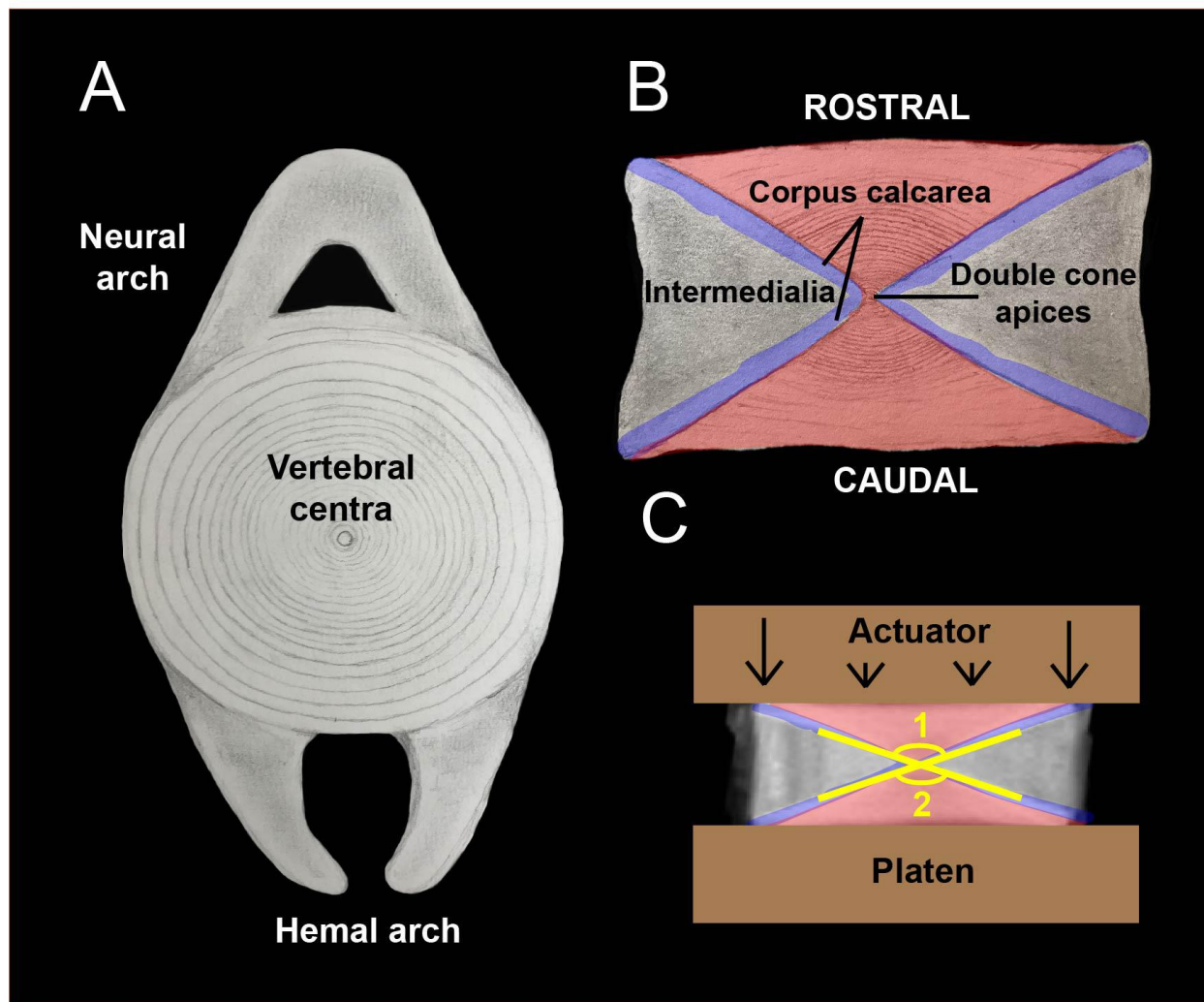
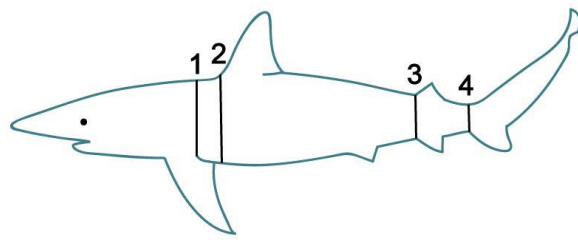
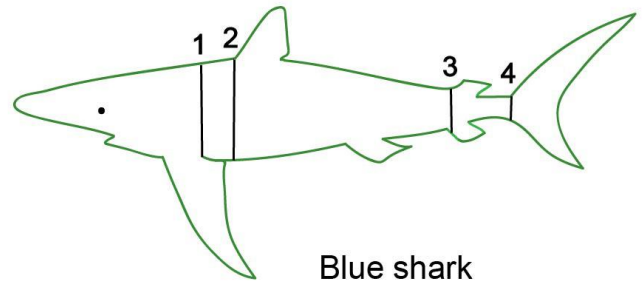


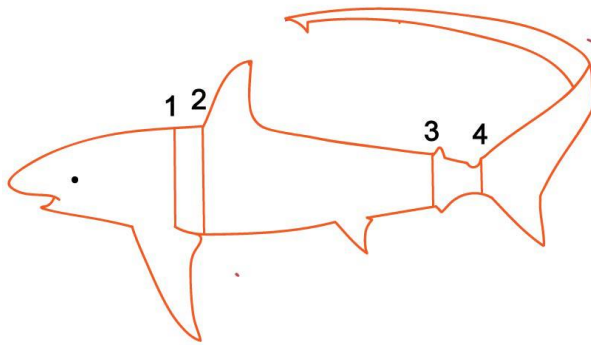
Figure 1. Anatomy of shark vertebral centra. (A) Frontal view of a centrum details mineralized concentric rings that extend out toward the centrum edge. The neural arch extends dorsally in the shark and the hemal arch, which is present in the caudal region only, extends ventrally. (B) Sagittal view of a cross-sectioned centrum detailing the double cone structure with apices pointing towards the center. The intermedialia (red) and corpus calcaria (blue) make up the mineralized double cone structure. (C) Centra were subjected to quasi-static compression tests. From centra x-rays (sagittal view), the area of double cone (blue- intermedialia plus the red- corpus calcaria) was quantified in addition to the angles formed at the double cone apices (yellow). Panels A and B: drawings by D.N. Ingle.



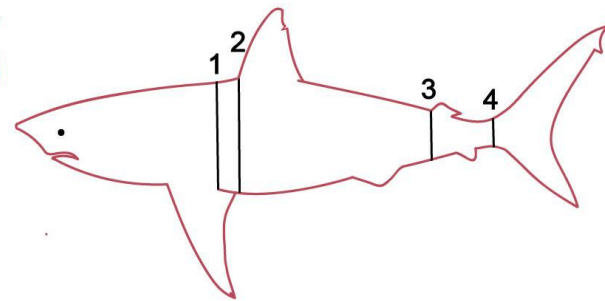
Dusky shark
(*Carcharhinus obscurus*)



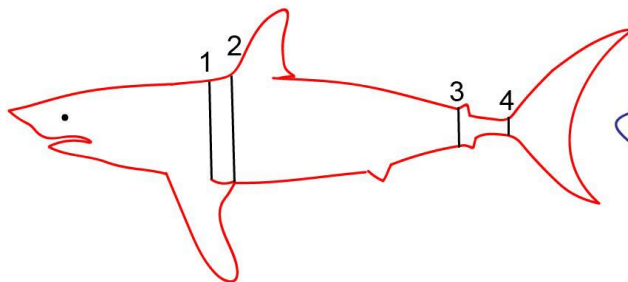
Blue shark
(*Prionace glauca*)



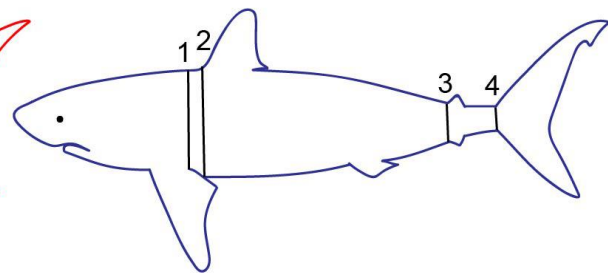
Common thresher shark
(*Alopias vulpinus*)



White shark
(*Carcharodon carcharias*)



Shortfin mako
(*Isurus oxyrinchus*)



Porbeagle
(*Lamna nasus*)

Figure 2. Vertebrae were sampled from four locations in six shark species: (1) the pectoral fin insertion, (2) the first dorsal fin origin, (3) the second dorsal fin origin, and (4) the pre-caudal pit. For this study, three vertebrae were sampled from each region per shark. For statistical analyses, mechanical properties from regions (1) and (2) were pooled together as the anterior region and properties from regions (3) and (4) were combined as the posterior body region.

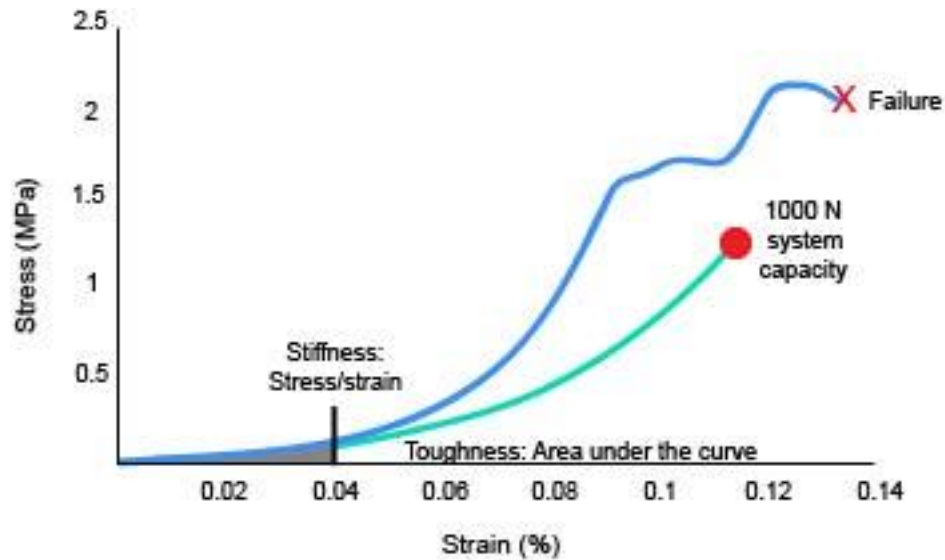


Figure 3. Stress-strain curve of cartilaginous centra tested in compression. These centra were aligned with the pectoral fin insertion in the small (74.5 cm TL, blue line) and large (226 cm TL, green line) dusky shark. The small shark centrum (blue line) demonstrates yield behavior and transitions into permanent deformation. The large shark centrum (green line) reached the 1000 N system threshold of the Instron E 1000 within the linear portion of the curve (denoted by the red circle). The gray shading denotes the area under the curve (toughness) and stiffness (stress/strain) at 4% centrum length deformation for the small dusky. Additional stress-strain curves of shark centra in compression are provided in Figure S1.

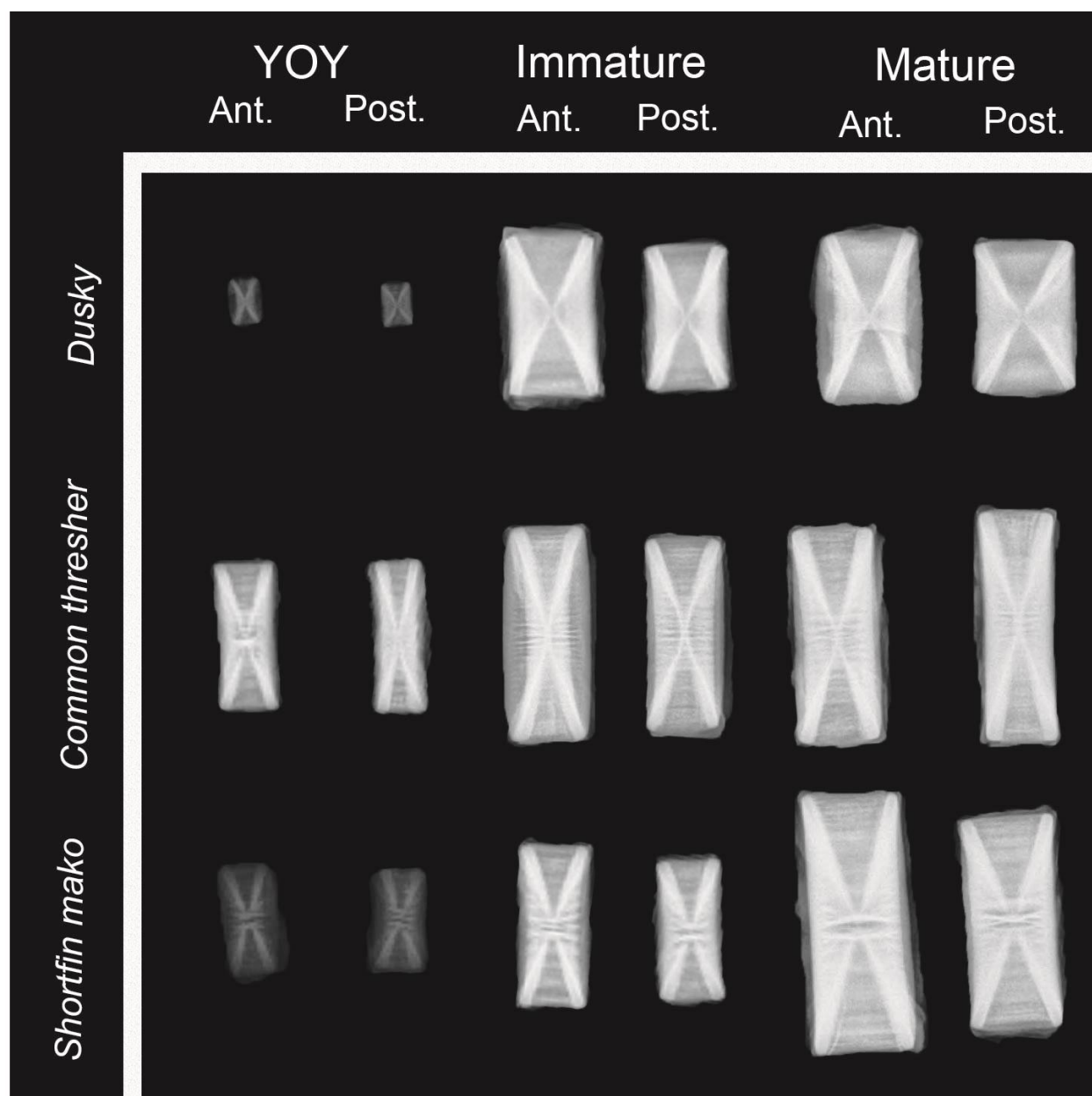


Figure 4. Variation in centra mineralization among regions, animal sizes, and species. Dusky, common thresher, and shortfin mako representatives of the three shark families sampled: Carcharinidae, Alopiidae, and Lamnidae; respectively. YOY (young of the year), immature, and mature denote the three animal developmental classifications. Anterior and posterior labels refer to centra aligned with the pectoral fin insertion and the second dorsal fin origin; respectively.

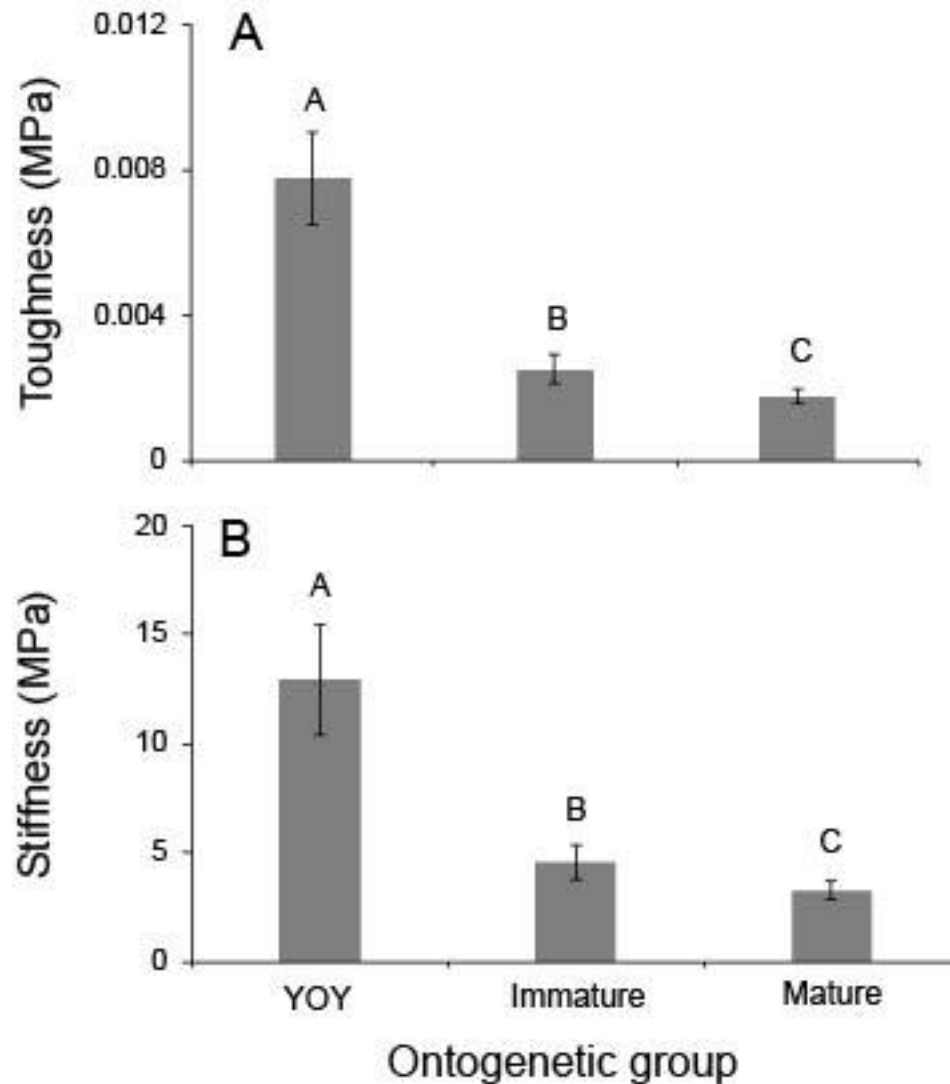


Figure 5. Centra mechanical properties among shark ontogenetic groups. (A) Centra toughness was greatest in YOY animals, mature shark centra was the least tough, and immature centra stiffness was intermediate ($P < 0.001$). (B) Stiffest centra were also from YOY sharks, while the least stiff centra was from mature sharks and immature centra fell between the two ontogenetic groupings ($P < 0.001$). Bars are means of ontogenetic groupings for shark species. Error bars denote \pm s.e.m. Note that y-axes for each mechanical property change among panels.

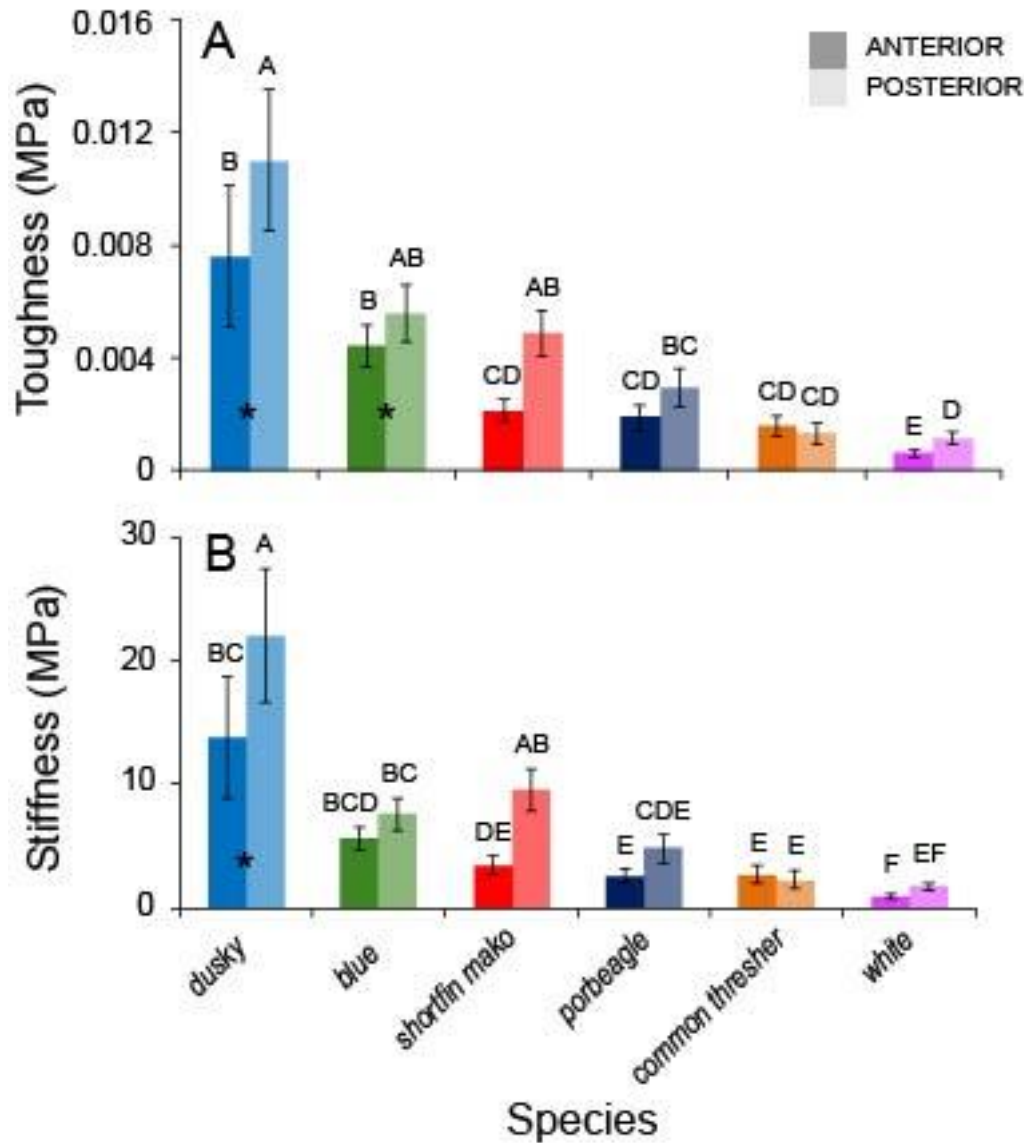


Figure 6. Centra mechanical properties from anterior (pectoral fin insertion and first dorsal fin origin: dark shade) and posterior (second dorsal fin and precaudal pit: slight shade) body regions among species. (A) Overall, centra from the posterior body were tougher than from the anterior body ($P < 0.001$). Species in which posteriorly-located centra were tougher than the anterior body were the dusky, mako, and white shark. (B) Similarly, overall centra stiffness was greatest in the posterior body ($P < 0.001$). Centra from the posterior vertebral column were significantly stiffer than the anterior region in the dusky and mako sharks. Bars are means of the two regions for each species. Error bars denote \pm s.e.m. Asterisks within the bar graphs denote species with the significantly greatest means. Letters above bars denote differences among anterior and posterior regions of each species.

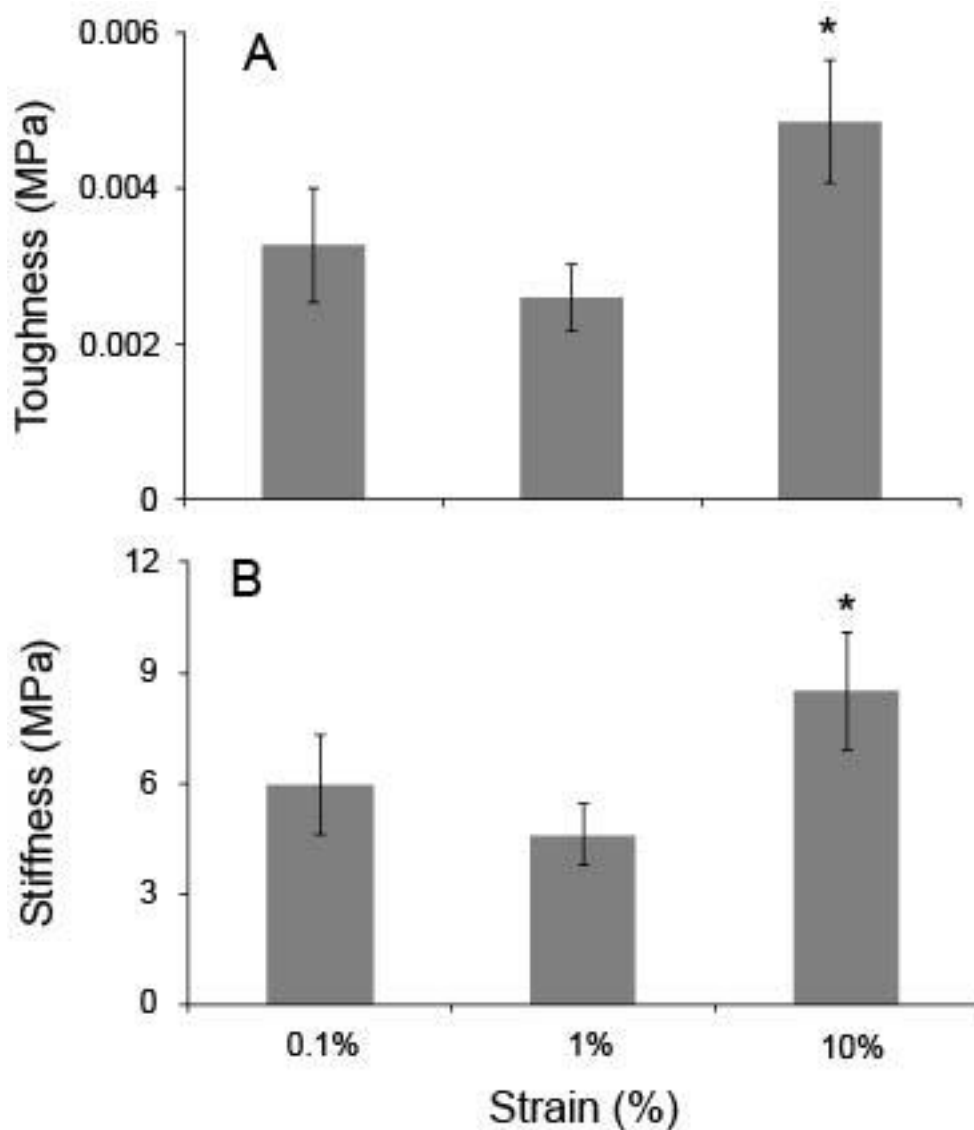


Figure 7. Centra mechanical properties among three strain groups. (A) Toughness at 10% strain was significantly greater than 1% and 0.1% strains among all samples ($P<0.001$). (B) Stiffness was also the greatest at 10% strain ($P<0.001$). Graph values are means for each strain rate. Error bars represent \pm s.e.m. Asterisks above bar graphs denote the statistically greatest mean.

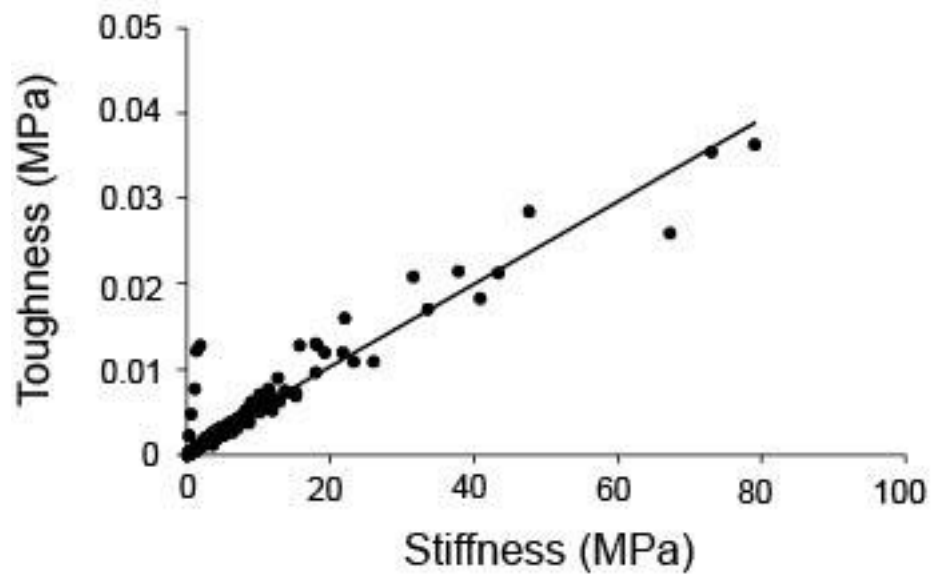


Figure 8. Regression of toughness by stiffness of all centra ($R^2=0.82502$, $P<0.001$). Doubling stiffness resulted in a nearly two-fold increase in toughness.

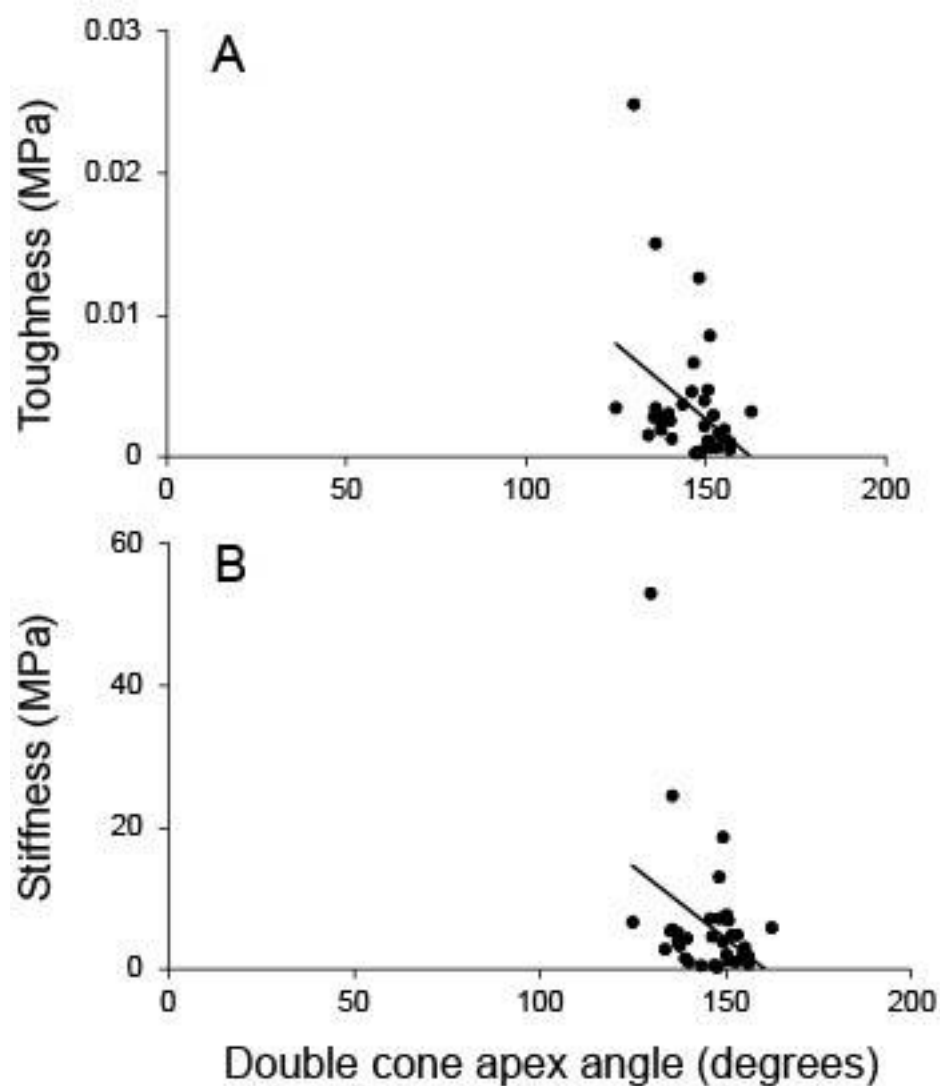


Figure 9. Regressions of mechanical properties by the angles formed at the double cone apex. (A) Centra toughness demonstrated an inverse relationship with double cone apex angle ($R^2=0.174903$, $P=0.0111$). (B) Stiffness also decreased with increasing apex angle ($R^2=0.182486$, $P=0.0094$).

Table S1. Average stiffness (MPa), toughness (MPa) and band pair counts of vertebral centra from mature sharks sampled for the present study and Natanson et al., 2018.

Species	Anterior (A and C)			Posterior (D and E)		
	Stiffness	Toughness	BP count*	Stiffness	Toughness	BP count*
Dusky shark (<i>Carcharhinus obscurus</i>)	3.9± 0.62	2.13e-3±3.93e-4	14.5±0.22	7.57±1.6	3.95e-3±7e-4	13.8±0.17
Blue shark (<i>Prionace glauca</i>)	5.18±1.43	2.88e-3±7.97e-4	14.4±0.5	3.8±0.62	2.25e-3±3.38e-4	15±1.29
Shortfin mako (<i>Isurus oxyrinchus</i>)	2.57±1.53	1.32e-3±7.58e-4	27.7±0.91	8.38±1.98	3.91e-3±9.46e-4	18±0.77
Porbeagle shark (<i>Lamna nasus</i>)	1.43±0.54	8.18e-4±2.66e-4	18.5±0.88	2.39±0.77	1.69e-3±3.71e-4	14.5±0.67
Common thresher shark (<i>Alopias vulpinus</i>)	0.78±0.15	4.93e-4±8.78e-5	21.5±0.56	1.15±0.22	6.4e-4±1.2e-4	18.8±0.75
White shark (<i>Carcharodon carcharias</i>)	0.35±0.08	2.2e-4±4.04e-4	25.27±1.6	0.89±0.24	5.27e-4±1.27e-4	16.3±0.61

Columns with (*) are data from Natanson et al., 2018

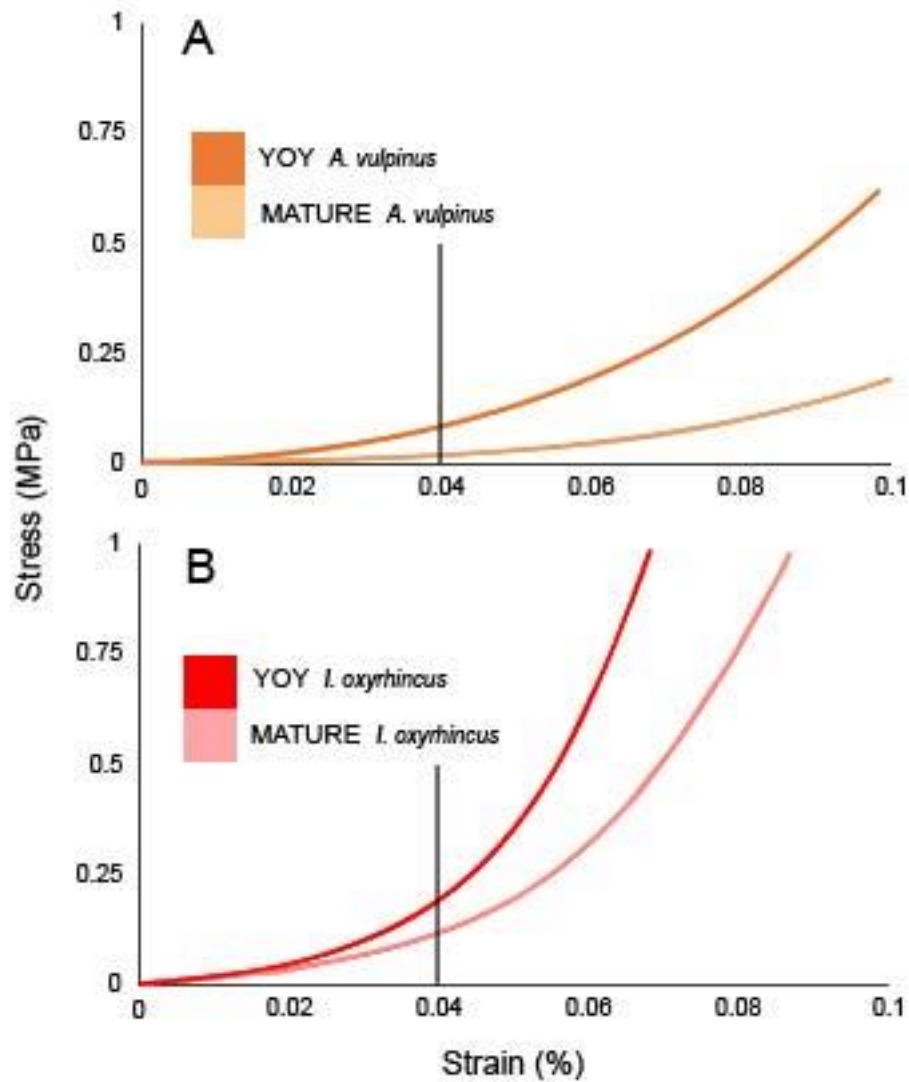


Figure S1. Stress-strain curves of YOY and mature shark centra that were compressed within the elastic (linear) region. 4% strain is the deformation in which stiffness and toughness were calculated. Curves detail data from compression tests from common thresher (A) and shortfin mako (B) and correspond with the x-radiographed YOY and mature shark centra from Figure 4. Dusky stress-strain curves are detailed in Figure 3.

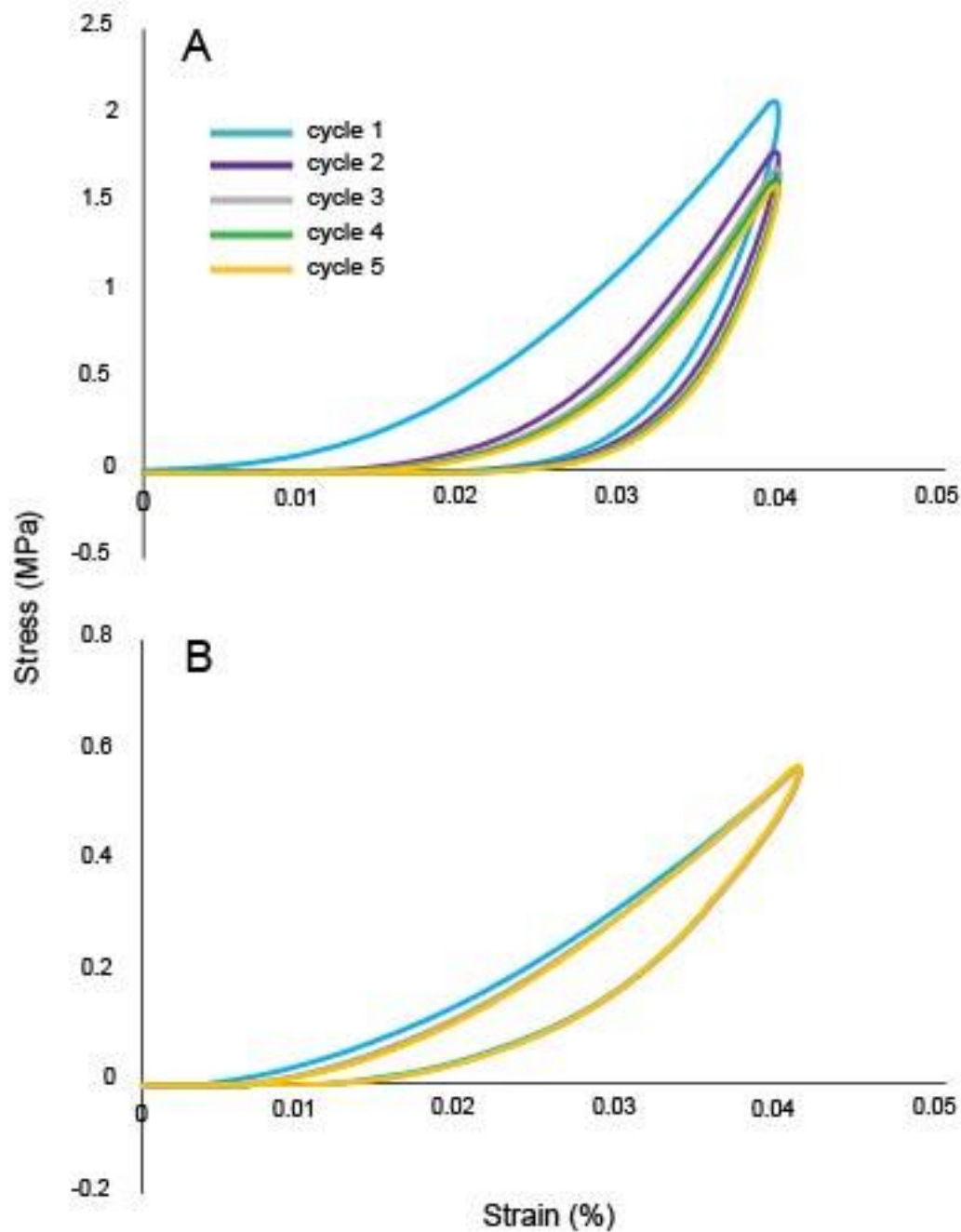


Figure S2. Cyclical tests (5) of centra from two mature sharks at a displacement rate of 0.03mm/s. (A) The centrum from a mature dusky had the following stiffness measures (MPa); cycle 1 = 50.66, cycle 2 = 44.14, cycle 3 = 40.2, cycle 4 = 40.36, cycle 5 = 39.57. (B) Common thresher had similar stiffness values among the five compression cycles; cycle 1 = 13.8, cycle 2 = 13.76, cycle 3 = 13.77, cycle 4 = 13.87, cycle 5 = 13.94.